Journal of The Korean Astronomical Society
41: 77 ~ 81, 2008 June

DEVELOPMENT OF A TOY INTERFEROMETER FOR EDUCATION AND OBSERVATION OF SUN AT 21 cm

Yong-Sun Park[1], Chang Hee Kim[1], Sang In Choi[2], Joo Young Lee[2], Woo Min Jang [2], Woo Yeon Kim[2], and Dae Heon Jeong[2]
[1] FPRD, School of Physics and Astronomy, SNU, Seoul, Korea
E-mail: yspark@astro.snu.ac.kr
[2] Gyeonggi Science High School, Suwon, Korea
(Received March 31, 2008; Accepted April 23, 2008)

ABSTRACT

As a continuation of a previous work by Park et al. (2006), we have developed a two-element radio interferometer that can measure both the phase and amplitude of a visibility function. Two small radio telescopes with diameters of 2.3 m are used as before, but this time an external reference oscillator is shared by the two telescopes so that the local oscillator frequencies are identical. We do not use a hardware correlator; instead we record signals from the two telescopes onto a PC and then perform software correlation. Complex visibilities are obtained toward the sun at $\lambda = 21$ cm, for 24 baselines with the use of the earth rotation and positional changes of one element, where the maximum baseline length projected onto UV plane is $\sim 90\lambda$. As expected, the visibility amplitude decreases with the baseline length, while the phase is almost constant. The image obtained by the Fourier transformation of the visibility function nicely delineates the sun, which is barely resolved due to the limited baseline length. The experiment demonstrates that this system can be used as a "toy" interferometer at least for the education of (under)graduate students.

Key words : instrumentation: interferometer — Sun: general — Sun: radio radiation — radio continuum: general

I. INTRODUCTION

In radio astronomy, an interferometer system including VLBI is virtually the only viable option to improve the angular resolution, because large single dish telescopes are expensive and technically difficult to construct, particularly at high frequencies. Therefore radio interferometer technology has been developed since the commencement of radio astronomy (Rolfs and Wilson 2000). The ALMA and KVN, which are under development, are the realization of the most recent interferometer/VLBI technology, the latter being the first large facility dedicated to mm VLBI observation.

In an attempt to assist (under)graduate students to become familiar with and understand interferometer systems, Park et al. (2006) have constructed a proto-type two-element radio interferometer and carried out the observation of the sun at a wavelength of 21 cm. They have measured only the amplitude of the visibility function, because each antenna has its own local oscillator and phase variations can not be correctly monitored. However, even without phase information, they were able to derive the brightness distribution of the sun, assuming axial symmetry.

The next step is to add the capability of measuring the visibility phase for full two-dimensional image synthesis. The easiest way to achieve this is to modify the local oscillator part of receivers so that an external reference signal is shared by the two telescopes.

In this paper, we report the realization of such a two-element interferometer and the observation of the sun using it. The system modification for attaining full functionality of measuring complex visibilities is described in section 2. Then, in section 3, we discuss the observation procedure and data reduction process to derive a two-dimensional image of the sun. Since the complex visibility is measured successfully, we are able to synthesize the solar image, which is described in section 4.

II. DEVELOPMENT OF INTERFEROMETER

(a) Strategy

We have developed a new interferometer, by modifying the receivers of the existing interferometer (Park et al. 2006). The interferometer is composed of two small radio telescopes (hereafter referred to as SRTs) with diameters of 2.3 m. The receiver is of the heterodyne type; thus the local oscillator downconverts a high frequency signal to a low frequency one. Detailed information on this telescope can be found at http://haystack.mit.edu/edu/undergrad/srt/index.html.

Corresponding Author: Y.-S. Park

In order to implement the capability of phase measurement, one should be able to monitor the phase difference between the two local oscillators. This phase difference is generally time varying and can be considered constant only within coherence time. However, each receiver of the existing interferometer has its own internal reference clock with an uncertain coherence time, to which the local oscillator is phase-locked. A solution to the phase jittering between the local oscillators is to measure the phase variation during observations, by using celestial point sources with a period shorter than the coherence time. However, no such sources are available because of the short exposure time of the developed system (see section 3 for detail). This was the reason why only the visibility amplitude could be measured in the previous experiment.

Another solution is to lock the reference oscillator of each telescope to a GPS time (or frequency) receiver. If this were accomplished, the interferometer would be similar to a VLBI. However, most GPS time receivers provide 10 MHz signal, whereas the reference signal in use is 8 MHz. The receiver could operate with 10 MHz; however, since the 8 MHz signal is also used as the basic clocks of other digital components in the receiver, it is difficult to change the reference frequency to 10 MHz. One could employ both the external 10 MHz clock for phase locking and the internal 8 MHz clock for other digital components; however, this would complicate the modification task.

Finally we have decided to use a low-cost 8 MHz quartz oscillator and feed its signal into the two SRTs via coaxial cables. Therefore, the final system becomes fairly similar to a conventional interferometer. One of the advantages of using a common external oscillator is that we do not need to fringe-fit the data.

(b) Modification of Receivers

As mentioned above, the local oscillator was originally phase locked to the internal 8 MHz clock using a frequency synthesizer chip. In order to replace it with an external clock, we first removed from the receiver board the internal clock (CR1) together with a resistor (R605) and a capacitor (C603) around the frequency synthesizer chip. Readers are referred to the receiver circuit diagram for the identification of the components (http://haystack.mit.edu/edu/undergrad/srt/receiver/Downloadable_Resources.html). Then an N-to-SMA flange adapter was mounted on the receiver box for directing external signals to the receiver and a coaxial cable was connected from the adapter to the position of the previous internal oscillator. In addition, a small 8 MHz external clock module was fabricated and cables with a length of 20 m were used to connect the external module and the receivers.

In the laboratory, we confirmed that the frequency synthesizer chip performs properly with the external clock, as it did previously with the internal one. In addition, we checked the phase stability of the receivers by comparing two output CW signals, for a common radio frequency (RF) signal applied to the receivers. The phase difference between the two CWs remained stable for a day.

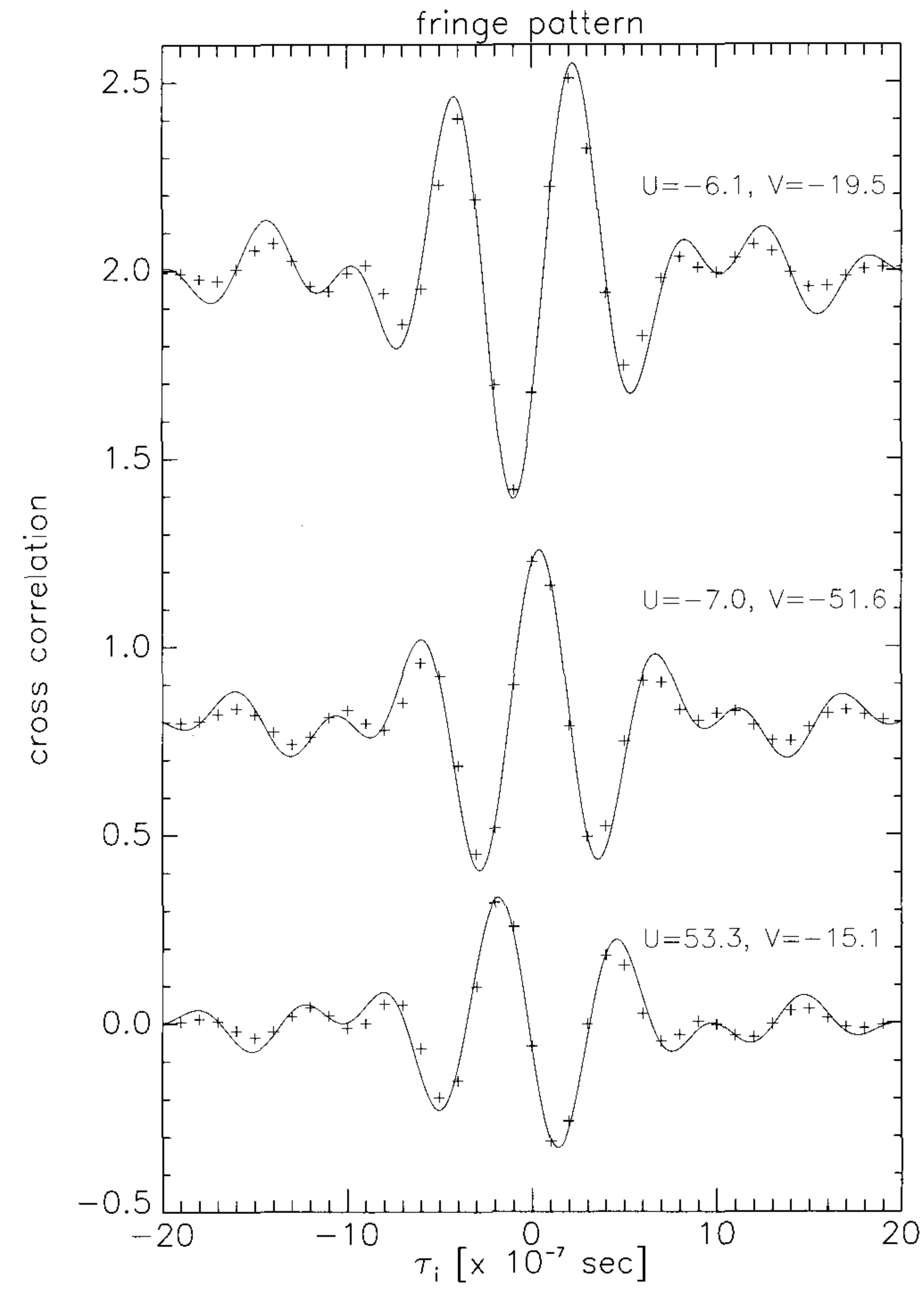

Fig. 1.— Examples of cross-correlations for various instrumental delays. The crosses denote data points and solid lines are fitted curve obtained by Eq. 1. They are arbitrarily shifted for clarity. U and V coordinates in units of wavelength at the time of observation are also shown. With these coordinates, one could find the corresponding locations in the UV plane shown in Fig. 4.

III. OBSERVATION

(a) Observation

After verifying the phase (difference) stability of the receivers, we carried out observations toward the sun from January 10, 2008, at the SRAO site of the Seoul National University campus. Here, we present the analysis result of the data collected from January 24 to 26, 2008. The adjusted 2.8 GHz solar flux, which is a measure of solar activity, was stable with 67−70 sfu during this period (http://www.drao-ofr.hia-

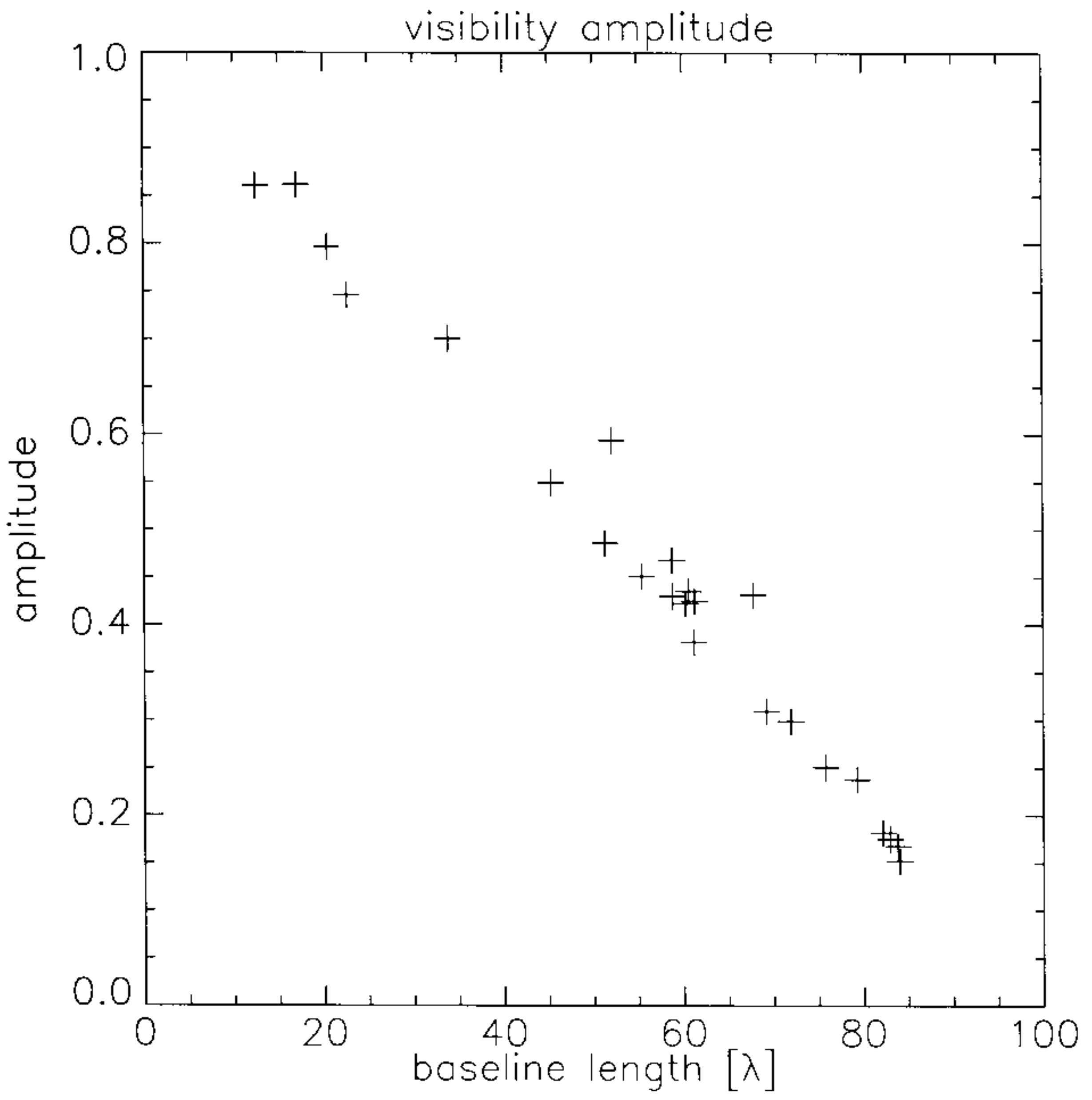

Fig. 2.— Variation of visibility amplitude with baseline length

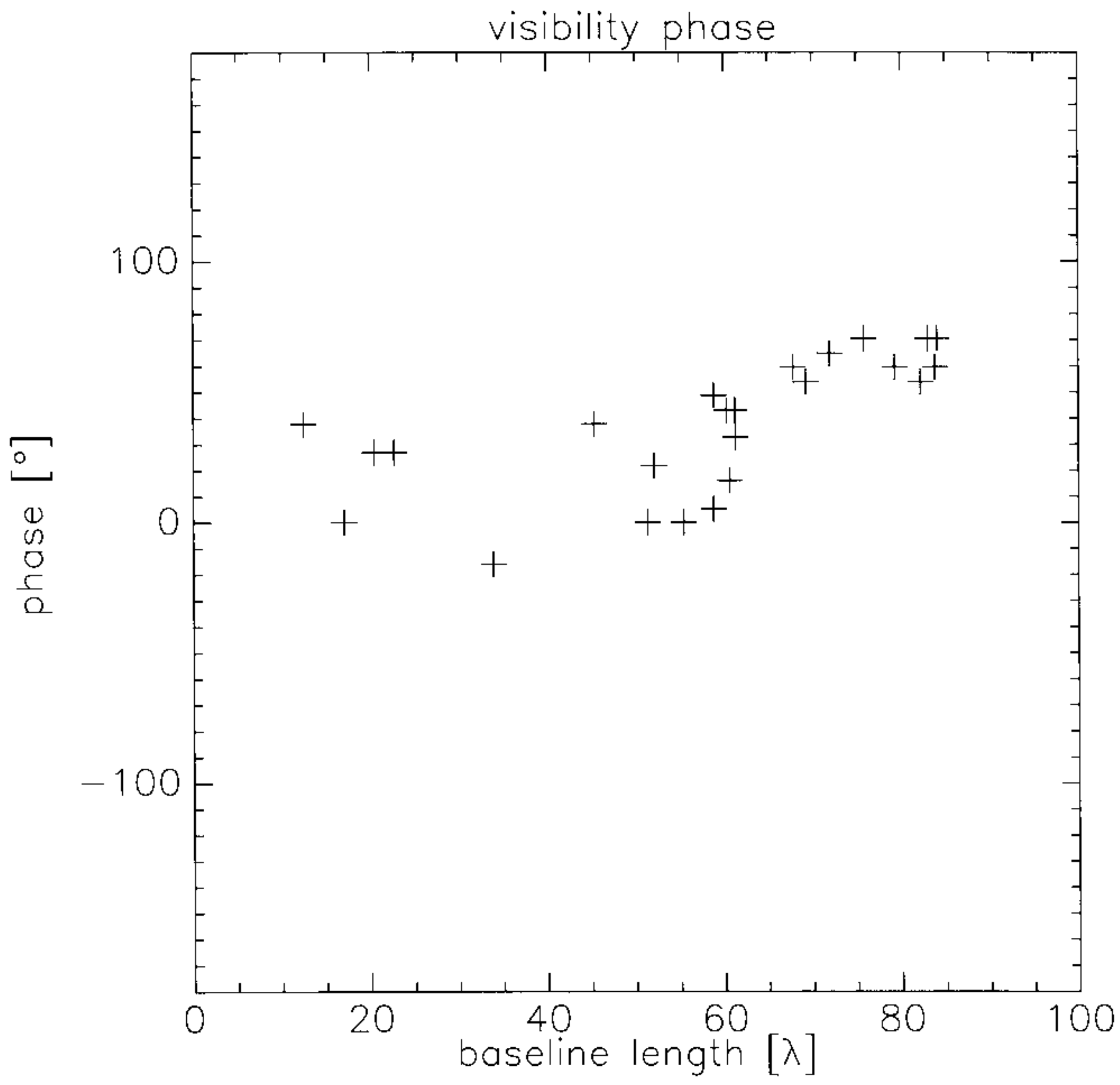

Fig. 3.— Variation of visibility phase with baseline length

iha.nrc-cnrc.gc.ca/icarus/www/sol_home.shtml). Thus we assume that the radio image of the sun does not change during observation.

We use the same data taking system described in the work by Park et al. (2006). Signals from the two SRTs, which are fed into a data acquisition card in a PC, are sampled and digitized at a rate of 10^7 samples s^{-1} and with an 8 bits resolution from −0.1 V to +0.1 V. The maximum number of samples is 10^6; therefore, the integration time is only 0.1 s. The integration time is sufficient for the observation of the sun; however, for the observations of any other objects, the integration time should be longer. The data are converted into text files whose size is ~ 11 MBytes per baseline and per telescope.

The local oscillator frequency is 1420.8 MHz and the intermediate frequency (IF) bandwidth is 1 MHz from 1 to 2 MHz. Since the SRT receiver operates in the LSB mode, the corresponding RF range is 1418.8 to 1419.8 MHz. In the single dish mode, the typical brightness of the sun is ~ 300 K in T_A^* unit and the system temperature is ~ 100 K.

On January 24 and 25, the two SRTs were fixed and the earth rotation was used to cover a certain range of UV plane. On January 26, one SRT moved to several locations so that the baseline vectors covered the regions of $U \approx 0\lambda$ and $V \approx -70\lambda$ to $V \approx 0\lambda$, where $\lambda = 21$ cm (see figure 4).

(b) Data Reduction

For a heterodyne receiver, a cross-correlation of the signals from the two SRTs in the LSB mode is given by the following equation for a rectangular passband (Perley et al. 1989):

$$r = A_0 \Delta\nu |V| \frac{\sin(\pi\Delta\nu(\tau_g - \tau_i))}{\pi\Delta\nu(\tau_g - \tau_i)} \times \cos[2\pi(\nu_{LO}\tau_g - \nu_{IF_0}(\tau_g - \tau_i)) - \phi_V - \phi_{LO}], \quad (1)$$

where $|V|$ is the amplitude of the complex visibility, $\Delta\nu = 1$ MHz is the IF bandwidth, τ_g is the geometric delay, τ_i is the instrumental delay, ν_{LO} is the local oscillator frequency, and $\nu_{IF_0} = 1.5$ MHz is the center frequency of the IF band. ϕ_V is the phase of the complex visibility and ϕ_{LO} is any phase difference between the local oscillator signals of the two SRTs. Although ϕ_{LO} is unknown, it is certainly constant. An addition of a constant term to ϕ_V does not affect image, and thus we derive $\phi_V + \phi_{LO}$.

The system temperature and the brightness of the sun in the single dish mode are almost constant over the observation period; thus we do not apply time- or elevation-dependent corrections to the data. Since we do not carry out flux calibration, the scale of the cross-correlation is rather arbitrary and accordingly, the scale of the solar image is arbitrary as well.

A crucial step of this experiment is to find fringes or interference patterns. After many trials and errors, we have successfully found the fringes, some of which are displayed in Fig. 1. Though there are several features

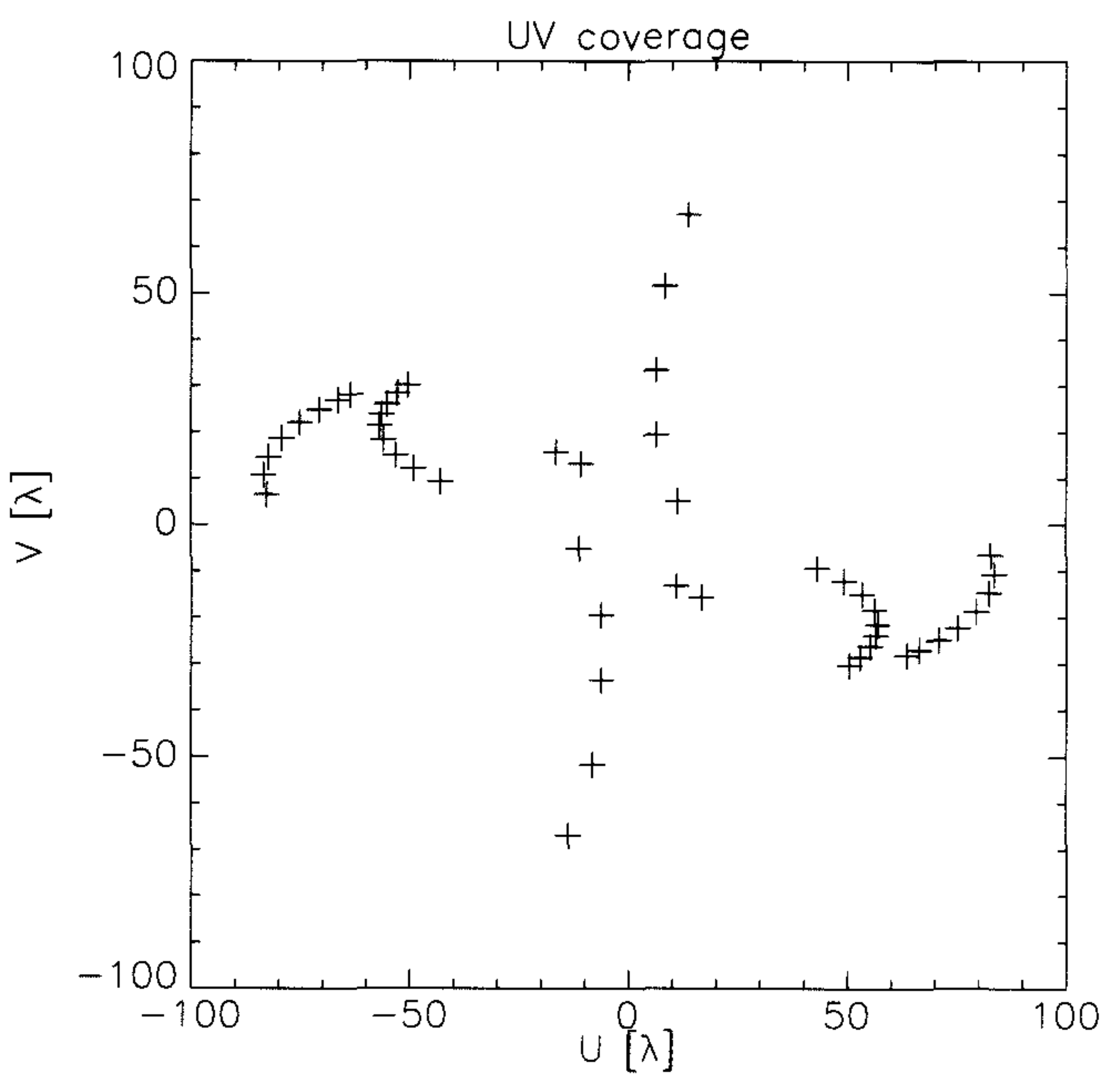

Fig. 4.— Projection of baseline vectors onto UV plane

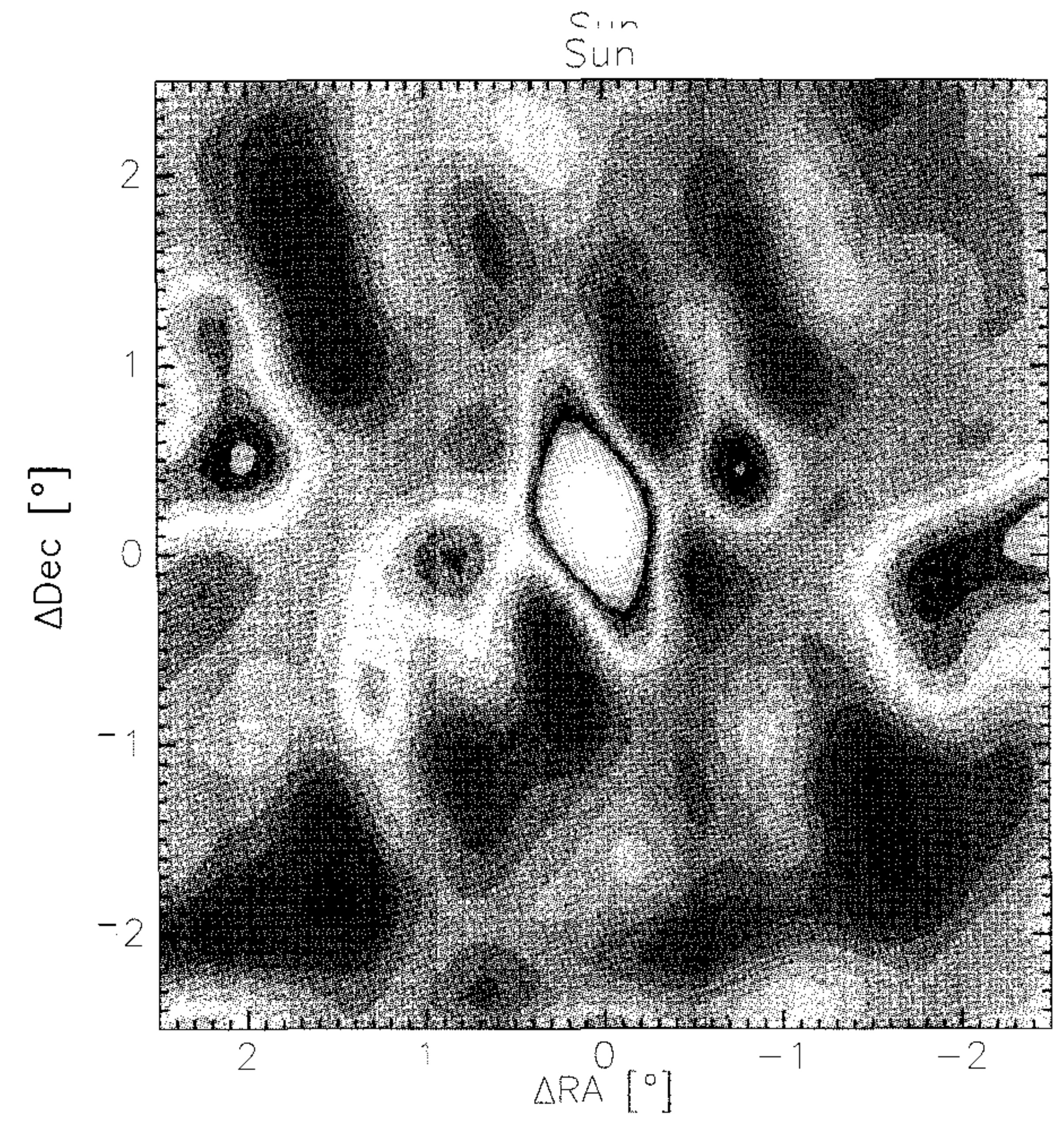

Fig. 5.— Synthesized image of the sun. Twenty contours of equal spacing are drawn from the minimum value of -0.35 to the maximum value of 1.

of artificial signals within the IF band, they have a negligible effect on the data. These data points are fitted to Eq. 1, in order to derive $|V|$ and $\phi_V + \phi_{LO}$. The fitting is overall satisfactory, and minor discrepancies may be due to the difference between the rectangular passband assumed in Eq. 1 and that of a real system.

In order to derive these quantities, we should know τ_g or delay length, which is the projected component of baseline vector onto the direction of phase tracking center. The required accuracy in the length measurement is $\lesssim \lambda/6$ or $\lesssim$ 3 cm. To obtain this accuracy, using a measuring tape, we first measure the position vectors of the two SRTs, with respect to a few reference positions on the ground. Then, coordinate transformations are made to express in the (U, V, W) coordinate system the baseline vectors which are the differences in the position vectors. The measurement accuracy is found to be 2 − 3 cm.

IV. RESULTS

By these steps, we are able to derive the complex visibility for the various baseline vectors. Fig. 2 shows the distribution of the amplitude of the visibility function as a function of the baseline length. Consistent with Park et al. (2006), the amplitude decreases as the baseline length increases.

Since the site is rather narrow, we can not observe the bouncing back of the amplitude at longer baselines observed by Park et al. (2006). The maximum baseline length indicates that the angular resolution is $\approx 0.5°$.

The distribution of the visibility phase is shown in Fig. 3, where the phase increases slightly with the baseline length. However, since its variation is within 1 rad rms, it can be considered to be approximately constant. This is a characteristic of point sources or sources with a symmetric brightness distribution at the phase tracking center.

We show the UV coverage of this experiment in Fig. 4, where the maximum baseline lengths are $\approx 90\lambda$ and $\approx 70\lambda$ in the U and V directions, respectively.

With these complex visibilities, we have synthesized a solar image using FFT, which is shown in Fig. 5. The image quality is good enough to discern the sun. The FWHM sizes of the sun are $\approx 0.5°$ and $\approx 0.8°$ in the east-west and north-south directions, respectively. The sun is located close to the center of the image; however, the peak position appears to be shifted to the north by 0.2°. The reason for this shift is unclear; however, there is a possibility that the shift is caused by errors in the measurement of the baseline vectors.

V. DISCUSSION AND SUMMARY

Since the angular resolution is just $\sim 0.5°$, we have been unable to observe limb brightening (Rohlfs and Wilson 2000; Park et al. 2006). However, the synthetic image of the sun demonstrates that the interferometer composed of the two SRTs performs well, even though it is fairly simple and primitive. This simple interferometer could be used to educate (under)graduate students.

One could further conduct heuristic programs, based on this experiment. The first one is to process the data in the spectrum mode. Even though there will be no spectral features, this could be a good exercise to understand how the interferometer works in the spectrum mode. The second one is to deal with the data after digitizing them to only two or three levels. With this program, one will experience the pros and cons of the digitization, such as fast processing and quantization noise (Thompson et al. 1986).

Further improvements could be suggested in terms of UV coverage, integration time, processing speed, and image quality. For example, the construction of a hardware correlator will make it possible to integrate longer for the observations of weak sources. Combining more elements will definitely ensure the images of better quality, though it is accompanied by complexities.

ACKNOWLEDGEMENTS

This work was supported by the 2007 R&E Program of Ministry of Science and Technology.

REFERENCES

Rohlfs, K. & Wilson, T. L., 2000, Tools of Radio Astronomy, Springer-Verlag

Thompson, A. R., Moran, J. M., & Swenson, G. W., 1986, Interferometry and Synthesis in Radio Astronomy, John Wiley & Sons

Perley, R. A., Schwab, F. R., & Bridle, A. H., 1989, Synthesis Imaging in Radio Astronomy, Astronomical Society of the Pacific

Park, Y.-S. et al., 2006, Development of Semi-VLBI System and Observation of Sun at 21 cm, JKAS, 39, 51